Journal of Inclusion Phenomena **6** (1988), 193–211.

Vanadyl Phosphate Dihydrate, a Solid Acid: The Role of Water in $VOPO_4 \cdot 2H_2O$ and its Sodium Derivatives $Na_x(V^{IV}_x V^{V}_{1-x} O)PO_4 \cdot (2-x)H_2O$

NIEVES CASAÑ*, PEDRO AMORÓS, RAFAEL IBAÑEZ, EDUARDO MARTÍNEZ-TAMAYO, AURELIO BELTRÁN-PORTER, and DANIEL BELTRÁN-PORTER**
UIBCM, Departamento de Química Inorgánica, Facultad de Químicas, Universitat de València, Dr. Moliner 50, 46100-Burjassot (València), Spain

(Received: 29 June 1987; in final form: 18 November 1987)

Abstract. Sodium-containing intercalates having as general formula $Na_xVOPOP_4 \cdot (2-x)H_2O$ ($0.25 \leqslant x < 0.50$) have been obtained and characterized. Orthorhombic phases, which essentially maintain the structure of the layered oxide hydrate $VOPO_4 \cdot 2H_2O$ result. Intercalated sodium ions act as 'pillars'. The presence of H_3O^+ ions in the parent $VOPO_4 \cdot 2H_2O$ and also in some reduced phases, is detected. The understanding of the structural role of the water molecules is advanced and the topotactic dehydration/rehydration processes are studied. The formation of a new metastable $VOPO_4 \cdot H_2O$ phase is established.

Key words: Vanadyl phosphate, inclusion compounds, topotactic reactions, solid acids.

1. Introduction

Theoretical and applied interest concerning the V–P–O system has resulted in a plentiful literature on its constituent phases [1, 2]. In particular, vanadyl phosphate, $VOPO_4$, has been widely studied owing to its catalytic relevance [1, 3, 4]. Up to now, five different polymorphs have been reported, α_I [5], α_{II} [6], β [7], γ and δ [1]. Besides these, the dihydrate $VOPO_4 \cdot 2H_2O$ can be derived topotactically from the α-phases [8]. Both α-phases are tetragonal ($P4/n$) and layered, α_{II} being isostructural with several $MOXO_4$ compounds [9]. The *ab* plane in the α-phases consist of VO_6 pseudo-octahedra sharing in-plane corners with PO_4 tetrahedra. The distorted VO_6 octahedra form infinite linear chains parallel to the *c* axis by sharing the apical oxygen atoms. The structure of the dihydrate $VOPO_4 \cdot 2H_2O$ has been described based on a single-crystal X-ray study [10] and by powder neutron diffraction [11]. Although there is some disagreement between the results of both studies, "the general features of the structure are clearly established" [12]. The space group is conserved (with respect to the anhydrous α-phases), but a significant elongation of the *c* axis occurs. The octahedral-tetrahedral array in the tetragonal layers is essentially maintained, but the layers are now separated by intercalation of water molecules. One water molecule (type A) is directly coordinated to a vanadyl group (V=O) and the second one (type B) is inserted into holes between PO_4 tetrahedra of adjoining layers, although the real position and local symmetry of both water molecules have not been exactly determined [13, 4]. In fact, besides the insensitivity of neutron diffraction to the vanadium atom, hydrogen atom positions are not accurately determined (R factor = 0.19). This is probably due in part to the sample

* Current address: Chemistry Department, Georgetown University, Washington DC (U.S.A.).
** Author for correspondence.

preparation procedure (see the Experimental section for pressure effects). Otherwise, hydrogen atoms may have no definite equilibrium positions.

The dihydrate $VOPO_4 \cdot 2H_2O$ has been aptly described as a versatile host for intercalation chemistry and phenomenological aspects of coordination [9, 14] and redox [12, 15] reactions have been reported. However, some basic questions remain unresolved. Thus, it seems clear that a more fruitful study of the intercalation reactions could be approached if the dehydration/rehydration (deintercalation/intercalation) pathways were known. Likewise, these mechanisms could be better understood provided that the actual structural role of the water molecules is established.

To progress in this sense, the present study is intended to elucidate the influence of the intercalated species both from a structural point of view and on the reactivity of the host lattice.

2. Experimental

The main features concerning the synthesis of the host lattice and its reduced phases have been summarized in Table I. Solid phases have been prepared from an aqueous solution containing NaH_2PO_4 0.770M, $NaVO_3$ 0.134M and HNO_3 0.754M. The $V/P \simeq 0.2$ molar ratio corresponds to the highest observed yield. The 'dihydrate' host lattice (Solid **I**, see below) was obtained according to Jander's procedure [16]. Reduced derivatives have been obtained: (1) In homogeneous (liquid) phase. Ethanol (Solid **II**) and SO_2 (Solids **III–V**) were used as reducing agents. SO_2 was supplied as a fresh Na_2SO_3/HNO_3 solution (in such a way that the pH and the Na^+/NO_3^- ratio in the starting solution were not altered). After addition of the reducing agent, the solutions were heated to incipient boiling (this was maintained for 15 minutes for Solids **II** and **IV**) and then they were allowed to cool to room temperature. The green crystalline solids obtained were filtered under vacuum, washed with cold water and dried with ether (saturated with water); (2) By reduction of Solid **I** samples. Reduction was carried out thermally for Solids **VIII** and **IX** (samples of **I** were maintained at the indicated temperature – see Table I – for 2–3 hours and then they were allowed to cool to room temperature under the same O_2-free atmosphere). Solid **VII** was prepared by prolonged reflux of an ethanolic suspension of **I**. Solid **VI** was prepared by reducing a 0.40M aqueous solution of **I** with an equal amount of a 0.20M aqueous solution of NaI. The green crystalline solids were treated as above.

Vanadium content and oxidation states were determined by a redox titration procedure. Samples were dissolved in dilute sulfuric acid and the V(V) was reduced with an excess of Fe(II). The solution was then back-titrated with standardized MnO_4^-. The procedure was carried out under a CO_2 atmosphere at 85 ± 1°C. End points were determined potentiometrically using a Pt/Calomel PK-149 Radiometer redox electrode. Phosphorus was determined by atomic absorption (Perkin-Elmer Zeeman 5000) and Na using an EEL Flame Photometer. Water was determined thermogravimetrically. The formulations in Table I have been proposed on the basis of the analytical results.

Thermogravimetric analyses were performed using a Setaram 870 simultaneous TG-DTA thermobalance. Crucibles containing *ca.* 100 mg of sample were heated at 4.43°C min^{-1} under a flowing N_2 atmosphere. The heating rates for the kinetic measurements were slower, ranging from 0.83 to 1.80°C min^{-1}. Calcined Al_2O_3 was used as reference.

X-Ray powder diffraction patterns were obtained with a Kristalloflex 810 Siemens diffractometer using Cu $K\alpha$ radiation with the Pt peaks as standard. The apparatus is

Table I. Synthesis of vanadyl phosphate dihydrate and some reduced phases

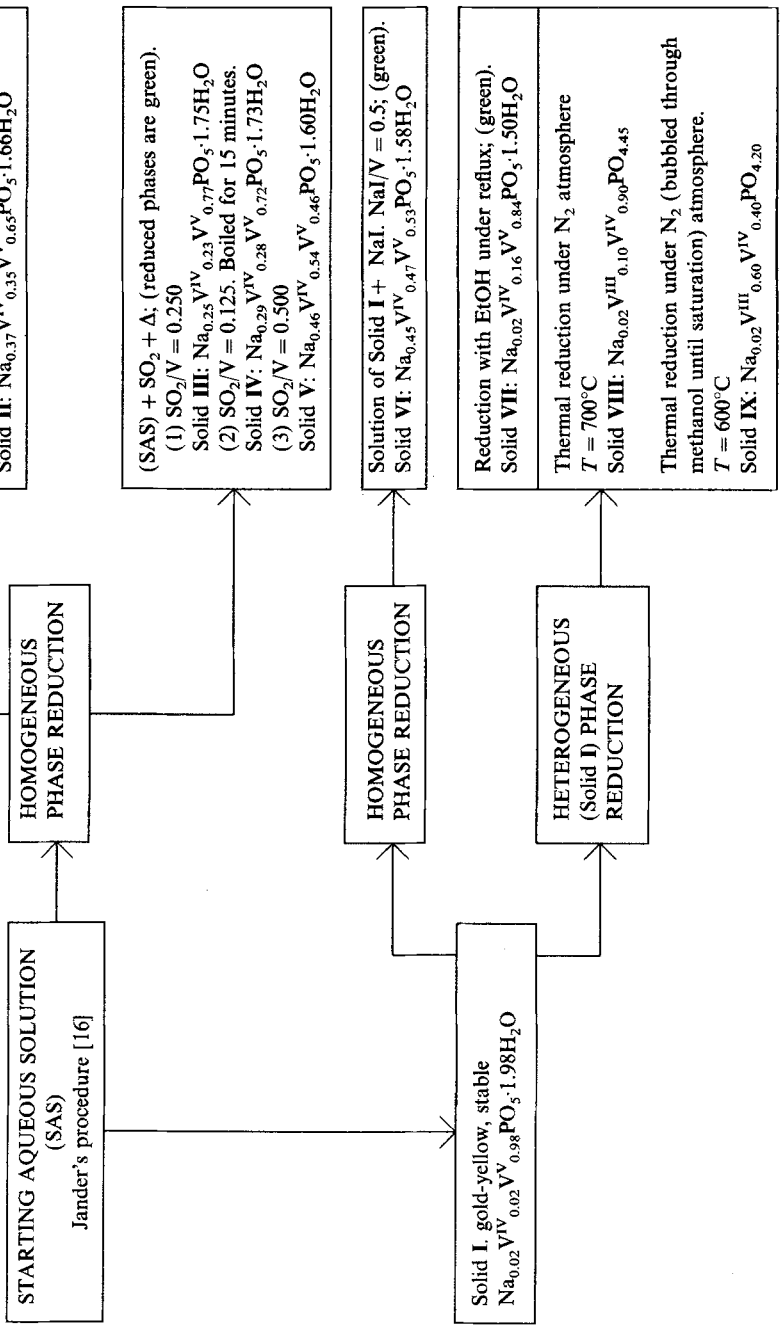

equipped with a variable temperature device working from room temperature to *ca.* 1200°C. During sample handling, even moderate pressures must be avoided. Partial decomposition to V_2O_5 is detected by spectroscopy and X-ray diffraction at pressures as low as 2.9 KBar. The sample-layer morphology confers a strong tendency to show a preferential orientation. We have made use of this to obtain simplified diffraction patterns in the variable temperature study.

IR spectra (KBr pellets made at low pressure) were recorded on a Pye Unicam SP 2000 Spectrophotometer. Polycrystalline powder EPR spectra were obtained on a Bruker ER 200 D X-band spectrometer.

3. Results and Discussion

3.1. SYNTHESES

Examination of Table I shows that the nature of the sodium intercalates described here depends strongly on the preparative procedure. Thus, heterogeneous phase reduction (i.e., processes analogous to those reported as "redox intercalation" [12]) can yield mixed solid phases in which the fraction of vanadium(V) reduced is higher than the degree of sodium intercalation (Solids **VII–IX**). In contrast, when working in an homogeneous medium (aqueous solution), the Na/V(IV) ratio in the reduced phases is always close to 1/1 (Solids **II–VI**). This last method (through reactions which are not intercalation reactions) is clearly advantageous because homogeneous solid single phases (see below) are obtained. Our results agree with the previous suggestion on the existence of an upper limit to the amount of sodium that can be intercalated in the host lattice [12, 15]. Although kinetic factors are important (e.g., **IV** is more extensively reduced than **III** despite the lower proportion of reducing agent used), neither boiling for longer times nor addition of an excess of reductant has allowed us to intercalate sodium in any amount higher than 46% of the total vanadium content in the host lattice. On the other hand, all attempts to obtain reduced single phases containing less than 25% of sodium have been unsuccessful, leading systematically to mixed phases or to the formation of the corresponding amount of Solid **III**. However, a remarkable feature is that, contrary to previous reports [12], the water content in the lattice (see Table II) lessens as the proportion of V(IV) (and consequently the Na^+ intercalated) increases.

Solids **III**, **IV** and **V** were investigated for the presence of SO_4^{2-} (with Ba^{2+} in neutral solutions) and/or SO_3^{2-} (nitroprussate test) always giving negative results. The IR spectrum of **II** rules out the presence of intercalated ethanol. The stoichiometries of **II**, **III** and **IV** indicate a $V(IV)/Na^+ = 1/1$ molar ratio. The presence of two weak bands (bending PO—H, 1375 cm^{-1}, sharp; ν(PO—H), 2322 cm^{-1}, broad [17]) in the IR spectrum of **V**, supports proton insertion in order to compensate for the positive charge defect (due to the upper limit to sodium intercalation).

As can be seen, Solid **I** contains a slight amount of Na(2% of **V** is V(IV)). This is a systematic result when Jander's procedure is used. A vanadyl phosphate practically free of V(IV) can be prepared in the absence of Na using the Ladwig procedure [18] as modified by Martinez *et al.* [14]. Notwithstanding, Solid **I** (which is indefinitely stable if preserved from light) behaves almost identically to the true dihydrate compound. Thus, its X-ray diffraction pattern (see Table III) practically coincides with that reported in the literature for $VOPO_4 \cdot 2H_2O$ [2].

Table II. Anaytical results

Solid	Na/V_{total} (molar ratio)	$V(IV)/V_{total}$ (molar ratio)	H_2O/V_{total} (molar ratio)	Dehydration			
				1st Step		2nd Step	
				n_w**	T (°C)*	n_w**	T (°C)*
I	0.02	0.02	2.00	1.01	104	0.99	144
III	0.25	0.23	1.75	0.99	144	0.76	193
IV	0.29	0.28	1.73	0.99	147	0.74	184
II	0.37	0.35	1.66	0.98	140	0.68	184
VI	0.45	0.47	1.58	1.00	140	0.58	188
V	0.46	0.54	1.60	1.01	124	0.59	188
VII	0.02	0.16	1.50	0.88	108	0.62	160
VIII	0.02	0.10	—	—	—	—	—
IX	0.02	0.40	—	—	—	—	—

* Endothermic peak temperature. ** Water molecules evolved.

Table III. X-ray powder diffraction data. The amount of intercalated sodium increases from left to the right (the Na/V molar ratio is given in parentheses)

Solid **I** (0.02)			Solid **III** (0.25)			Solid **IV** (0.29)			Solid **II** (0.37)			Solid **VI** (0.45)			Solid **V** (0.46)		
$d_{obs.}$	I/I_0%	*hkl*	$d_{obs.}$	I/I_0%	*hkl*	$d_{obs.}$	I/I_0%	*hkl*	$d_{obs.}$	I/I_0%	*hkl*	$d_{obs.}$	I/I_0%	*hkl*	$d_{obs.}$	I/I_0%	*hkl*
8.27	—	110**	7.52	10	011	7.47	10	011	7.52	—	011	7.49	2	011	6.55	100	002
7.47	100	001	6.75	100	002	6.71	100	002	6.77	100	002	6.55	100	002	5.25	10	102
4.78	10	121	4.59	10	112	5.38	1	012	5.27	6	102	5.25	1	102	4.41	5	200
4.41	—	040	4.33	2	200	5.32	6	102	4.55	12	112	4.59	3	112	3.91	5	103
4.12	—	220**	4.03	2	013	4.58	12	112	4.28	6	021	4.43	9	*	3.27	15	004
3.72	30	002	3.99	2	103	4.38	1	200	3.97	6	103	4.39	11	200	3.14	20	220
3.45	—	102**	3.37	15	004	3.98	5	103	3.38	20	004	3.91	10	103	3.07	17	014
3.19	3	240	3.13	30	220	3.35	25	004	4.13	50	104	3.27	36	004	2.99	15	030
3.11	10	300	3.07	15	221	3.17	—	023	3.07	25	220	3.14	45	220	2.95	1	123
2.87	3	212	3.01	10	030	3.13	30	203	3.05	10	203	3.10	29	203	2.88	10	301
2.47	1	003	2.84	7	222	3.07	25	221	3.01	15	030	3.00	18	030	2.80	1	310
2.39	2	023	2.62	—	132	3.00	20	030	2.83	15	130	2.88	12	301	2.84	10	222
2.30	5	322	2.50	—	033	2.84	10	222	2.77	5	131	2.77	8	131	2.72	1	032
2.23	—	133	2.46	3	230	2.77	—	131	2.69	5	005	2.72	1	311	2.62	1	204
2.20	—	203	2.24	—	125	2.72	10	311	2.65	5	204	2.63	2	204	2.57	—	312
2.11	—	143	2.17	5	106	2.66	10	204	2.50	5	033	2.40	3	321	2.51	1	015
2.00	—	153	2.10	2	410	2.50	—	033	2.43	5	230	2.34	1	313	2.46	1	320
1.97	—	441	1.99	—	234	2.30	—	322	2.19	8	016	2.18	12	140			
1.90	—	323	1.77	2	150	2.23	—	006	2.17	6	134	1.98	11	241			
1.86	—	004				2.19	—	400	2.15	4	304	1.96	9	324			
1.81	—	114				2.17	—	016	2.11	4	116						
1.78	—	034				2.14	—	314	1.98	10	240						
1.71	—	044				2.10	—	116	1.77	5	150						
							2.00	—	035								
							1.93	—	315								
$a = 9.35(1)$			$a = 8.38(3)$			$a = 8.67(1)$			$a = 8.76(1)$			$a = 8.79(4)$			$a = 8.82(1)$		
$b = 17.60(2)$			$b = 9.04(2)$			$b = 9.05(1)$			$b = 9.01(2)$			$b = 9.01(2)$			$b = 8.99(2)$		
$c = 7.45(2)$			$c = 13.55(2)$			$c = 13.51(1)$			$c = 13.43(1)$			$c = 13.11(4)$			$c = 13.10(2)$		

* peak not indexed. ** indexed peak with an orthorhombic cell. Cell parameters in Å.

The utilization of NaI as reducing agent illustrates the advantages of working in a homogeneous liquid phase. Thus, Solid **VI** is a single phase (see Table III) analogous to the above (**II–V**), but when working in a heterogeneous medium mixed phases can result [12].

3.2. THE ORTHORHOMBIC DISTORTION: THE ROLE OF INTERCALATED SODIUM

X-ray powder diffraction pattern data (Solids **I–VI**) have been summarized in Table III. Indexation and lattice parameter determination was performed by least squares fitting of the data in the range $10° < 2\theta < 50°$.

The pattern of Solid **I** is essentially like that reported for $VOPO_4 \cdot 2H_2O$ [2]. When indexed to a tetragonal structure, only three minor peaks remain unassigned (Table III) and the calculated lattice parameters ($a = 6.197(2)$ and $c = 7.417(2)$ Å) fit rather well with the previously reported values ($a = 6.21$ and $c = 7.41$ Å [2]). Nevertheless, indexation can be improved and we will return to this aspect later on.

The patterns of Solids **II–VI** correspond to five different single phases. However, indexation to tetragonal structures as made by Jacobson for the analogous intercalates [12] gives unsatisfactory results.

Actually, it seems reasonable to assume that replacing V(V) in the starting tetragonal lattice by V(IV) together with Na^+ insertion and H_2O evolution would induce a structural distortion. Thus, an accurate indexation has been possible for Solids **II–VI**, and even for **I** (holding as little as 2% V(IV)). In all cases, the best fit to the observed diffractograms is reached when an orthorhombic distortion is assumed. Indeed, for Solid **I** a full indexation is achieved for an orthorhombic cell having $a_r = a + b$, $b_r = 2a - 2b$ and $c_r = c$ (i.e., an orthorhombic cell having $a_r = 9.35(1)$, $b_r = 17.60(2)$ and $c_r = 7.45(2)$ Å). This multiple cell is similar to that proposed by Pulvin and Bordes for $AHVPO_6$ derivatives [21]. On the other hand, for Solids **II–VI** the best results are obtained when an orthorhombic distortion is assumed in such a way that the new a_r and b_r parameters are approximately equal to the diagonals of the hypothetical original tetragonal cell and c_r is about twice c (see Table III). The variation of the parameters yielding the best fit (see Figure 1) involves c_r lessening as the water content decreases (and simultaneously as the Na and V(IV) contents increase) and a_r increasing in the same sense. The b_r parameter remains practically unchanged with a value close to 9 Å. This value corresponds to the b parameter of the pseudo-orthorhombic cell for $VOPO_4 \cdot 2H_2O$ ($b_r = a\sqrt{2} = 8.76$ Å). As shown in Figure 1, a_r tends asymptotically to b_r.

As pointed out above, the c_r variation is related to the sodium and water content in the lattice. The thermal study (TG-DTA) of water evolution from these intercalates (see Table II) shows that: (1) water molecules are always lost in two stages; (2) the first one corresponds to the evolution of one water molecule per vanadium atom, regardless of the intercalation degree (x); and (3) the amount of water eliminated in the second stage approaches $(1 - x)$ molecules per vanadium atom.

In accordance with previous results reported for $VOPO_4 \cdot 2H_2O$ [2, 13], it can be assumed that the water evolved initially is that inserted into holes of the lattice (i.e., type B water). Therefore, the remaining water will be that directly coordinated to vanadyl groups. On this basis, and given the relation established between the intercalation degree (x) and the water content in the lattice, sodium ions in the intercalates are very likely replacing water molecules of type A (i.e., the sodium ions would be localized trans to the V=O bond of VO^{2+} reduced vanadyl groups). This way, the charge defect induced by the reduction should be neutralized locally. The resulting polyhedron of electronegative oxygen atoms

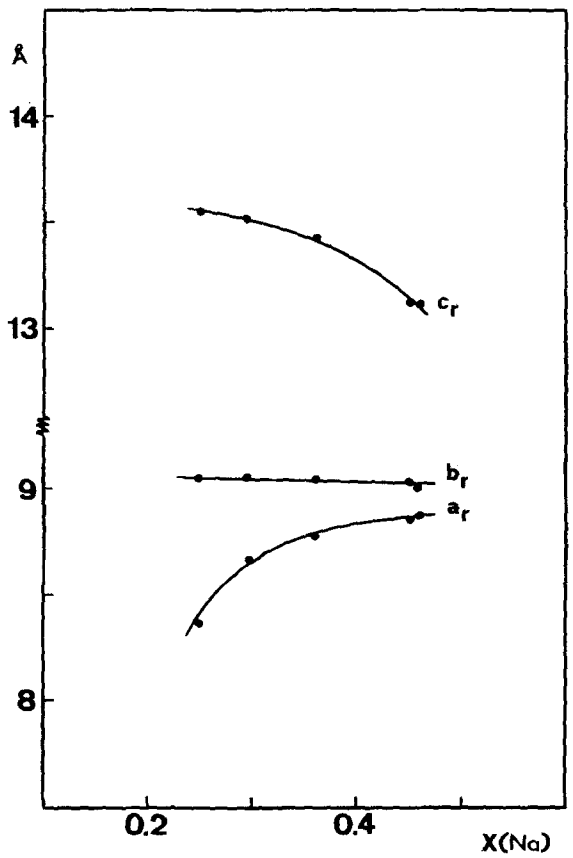

Fig. 1. Unit cell parameters as a function of the intercalation degree. Orthorhombic cell (*Pmma*) for $0.25 \leqslant x < 0.50$, and tetragonal cell ($P4_2mc$) for $x = 0.50$.

about each sodium cation would imply increased electrostatic interactions working to bring the layers closer. The *c* parameter decreases correspondingly. Thus, Na^+ ions may be considered as 'pillars' fixing adjacent layers by introducing ionic interactions in the Van der Waals gap. A similar effect has been observed for metal-complex intercalates [22] and also, in a very recent publication, for the intercalation of some di- and trivalent cations [23].

3.3. THE ORTHORHOMBIC DISTORTION: SPECTROSCOPIC RESULTS

The proposed tetragonal-orthorhombic-tetragonal structural evolution was first suggested by considering the IR spectral changes associated with intercalation (Table IV). Thus, the main features of the IR spectrum of tetragonal $VOPO_4 \cdot 2H_2O$ have already been described (see Table IV) [13]. From these, it can be inferred that the PO_4 groups should have an essentially C_{2v} local symmetry [24], which in turn agrees with the X-ray results [10]. The IR spectrum of Solid **I** is nearly coincident with the above. However, as the intercalation/reduction degree increases (Solids **II**–**IV**), a clear splitting of the δ_s(OPO) strong band is observed. Although less defined, there are no significant changes in the ν_{as}(PO) and ν_s(PO) bands. But, when the intercalated Na approaches the 'upper limit' (Solids **V**, **VI**), PO_4 bands appear again well resolved and δ_s(OPO) is unsplit. While this last result is consistent

Table IV. Infrared absorption wavenumbers (cm^{-1}) for $VOPO_4 \cdot 2H_2O$ and reduced phases. The amount of intercalated sodium increases from left to the right (the Na/V molar ratio is given in parentheses)

$VOPO_4 \cdot 2H_2O$ ref. [13]	Solid **I** (0.02)	Solid **III** (0.25)	Solid **IV** (0.29)	Solid **II** (0.37)	Solid **VI** (0.45)	Solid **V** (0.46)	Assignment
3620	3610 s	3609 sh	3600 s	3580 s	3540 s	3550 s	
3580	3520 m	3560 m	3530 w	3500 w	3480 w	3480 m	ν(OH)
3380	3330 s,b	3320 m,b	3330 m,b	3310 m,b	3344 m,b		
3120	3160 sh	3160 sh	3160 sh	3160 w,b	3170 m	3180 m,b	
	2940 w	2950 vw	2940 vw				$\nu_{as}(H_3O^+)$
	2870 w	2870 vw	2860 vw				$\nu_s(H_3O^+)$
						2322 m	ν(PO—H)
	2130 vw	2145 vw					ν(VO—H)
	1696 m	1690 w	1700 w	1695 vw			$\delta(H_3O^+)$
1625	1620 sh						
1610	1605 m	1615 m,b	1615 m,b	1615 m,b	1620 m,b	1620 m,b	δ(HOH)
						1375 w	δ(POH)
1170 w	1170 w	1170 w	1170 w	1175 m	1172 m		
1088 s	1085 vs	1087 vs	1090 vs	1090 vs	1080 vs		ν_{as}(PO)
1040 w	1035 w	1035 w	1040 w		1025 vs	1035 vs	
1000	980 sh	1000 sh	1000 sh	1000 sh	1000 w	1010 w	ν(V = O)
				987 sh	980 sh		
948 vs	950 s	965 m	950 m	955 m	955 vs	965 vs	ν(V—OH)
913 sh	910 m	911 w	905 sh	895 m	895 s	902 s	ν_s(PO)
875 sh	870 sh	872 w	875 sh				
685 w	685 w	680 w	680 w	690 w	680 w	680 w	δ(VOH) or δ(POH)
570 sh	575 w	560 w,b	562 w,b	540 w,b	535 w,b	535 w,b	δ_{as}(OPO)
401 s	410 s	405 s	403 s	400 s	400 s	400 s	δ_s(POP)
	390 s	395 s	395 s	385 s			
R(O—O) parameters.*							
3.61	3.65	2.98	2.96	2.92	2.76	2.75	R_1(O—O), Å
2.82	2.82	2.82	2.82	2.81	2.80	2.80	R_2(O—O), Å

* R_1(O—O), determined from crystallographic data ([10] and this work), measures the distance between the oxygen atom of a coordinated A water molecule and the oxygen atom of a vanadyl group of an adjacent layer; R_2(O—O), determinated from IR data using Pimentel's correlation [25], measures the distance between the oxygen atom of a coordinated A water molecule and the oxygen atom to which it is linked through an hydrogen bond.

with a C_{2v}-PO_4 local symmetry, the splitting of δ_s(OPO) in the spectra of Solids **II–IV** indicates a lowering of symmetry for the PO_4 groups, which become C_1 [24]. The C_{2v}(**I**)–C_1(**II–IV**)–C_{2v}(**V–VI**) change must be related to the noted structural evolution. Otherwise, for high degrees of reduction (Solids **V, VI**) the presence of both VO^{3+} and VO^{2+} entities is shown by the splitting of the ν(V=O) band.

The presence of V(IV) even in Solid **I** is illustrated by its anisotropic EPR spectrum (room temperature) displaying hyperfine structure ($g_{\parallel} = 1944$, $g_{\perp} = 1.984$, $A_{\parallel} = 194$ G, $A_{\perp} = 73$ G). These results are very similar to those reported for 'pure' $VOPO_4 \cdot 2H_2O$ [4]. EPR spectra of Solids **II–VI** remain axial but the hyperfine structure disappears because the dipolar and exchange interactions due to the increased V(IV) concentration.

3.4. THE INTERCALATED WATER

3.4.1. *Reduced Phases*

According to the IR spectra of Solids **I–VI** (Table IV), two water molecule types (A, coordinated, and B, inserted) occur in all the reduced phases. Bands at 3610, 3520 and 1605 cm^{-1} (Solid **I**) can be assigned to ν_{as}(OH), ν_s(OH) and δ(HOH) vibrations of A-type water molecules, respectively. Bands at 3350, 3160 and 1620 cm^{-1} (Solid **I**) can be assigned to ν_{as}(OH), ν_s(OH) and δ(HOH) vibrations of B-type water molecules, respectively.

Upon reduction, ν_{as}(OH) and ν_s(OH) remain split and a slight decrease in the frequencies assignable to A-molecules is observed. This can be related to the stronger coordinated water-substrate interactions resulting from the associated interlayer space shortening (see Section 3.2). Thus, from the data in Table IV it can be inferred that linear V—$O_{W(A)}$—H—O=V hydrogen bonds are reinforcing the interlayer forces when the amount of intercalated sodium increases. This conclusion is also supported by the observation of only one broad δ(HOH) band. The strengthening of the hydrogen bonds would increase the bending frequency [26]. This would lead to the overlapping of both A and B δ(HOH) bands.

Given that both water molecule types remain in the reduced phases, the understanding of their structural role might be approached by working with the starting-material (Solid **I**).

3.4.2. *The 'Monohydrate' Phase*

It may be thought that information on the A molecules could be provided by studying a monohydrate phase containing only coordinated water. While making such a study, Livage and coworkers have reported some interesting results [13]. They conclude that the coordinated water molecules in the monohydrate have C_s local symmetry and are arranged having the pseudo-C_2 axis approximately perpendicular to the layers. This model coincides with that proposed by Bruque *et al.* for $NbOPO_4 \cdot nH_2O$ ($n \sim 1$) [27]. Whereas our experimental results agree essentially with that of Livage, some refinements are indicated. The IR spectrum of the 'monohydrate' shows two strong bands at 3650 and 3555 cm^{-1} (3630 and 3540 cm^{-1} in [13]) which are assignable to ν_{as}(OH) and ν_s(OH) vibrations of coordinated water, respectively. However, there are also two very weak sharp bands at 3610 and 3520 cm^{-1} (3603 and 3518 cm^{-1} in [13]). These two bands, not discussed in [13], coincide with those observed for the coordinated A-molecules *in the dihydrate* (see Section 3.4.1). This result is a first indication of the different structural role of the coordinated water in the 'monohydrate' with regard to the dihydrate phase. Therefore, the decrease in the ν(OH)

frequencies upon further hydration must be attributed to the occurrence of hydrogen bonding interactions with the incoming B inserted water. Moreover, a broad weak band around 3330 cm^{-1} (*ca.* 3350 cm^{-1} in [13]) shows the presence of a slight amount of B water molecules in the formally 'monohydrate'. Accordingly, it can be concluded that, regardless of the preparative procedure, *the stoichiometric monohydrate phase* always contains a certain amount of inserted water molecules (see also Section 3.5). In any case no conclusion regarding the symmetry and orientation of the coordinated molecules in the 'monohydrate' is extrapolatable to the dihydrate phase.

3.4.3. *The Dihydrate Phase*

Dealing with the dihydrate, our results on the band dichroism support the fact that the orientation of the coordinated water molecules changes with respect to the structure proposed for the stoichiometric monohydrate phase. Because the experimental data are similar to those reported in [13], we do not include them here, but a comment is necessary. Thus, contrary to the observed data for the 'monohydrate', there are the bands due to ν_{as}(OH) and δ(HOH) which now become dichroic (both for A- and B-type water molecules), whereas just the band due to ν_s(OH) loses its dichroism.

On the other hand, we have recorded the IR spectrum of samples resulting from rehydration of α_1-$VOPO_4$. Rehydration was performed in a sealed flask in the presence of a $D_2O/H_2O = 5/95$ mixture. This low D_2O concentration ensured that only HOD molecules will replace H_2O molecules in the host lattice and also avoids problems arising from the

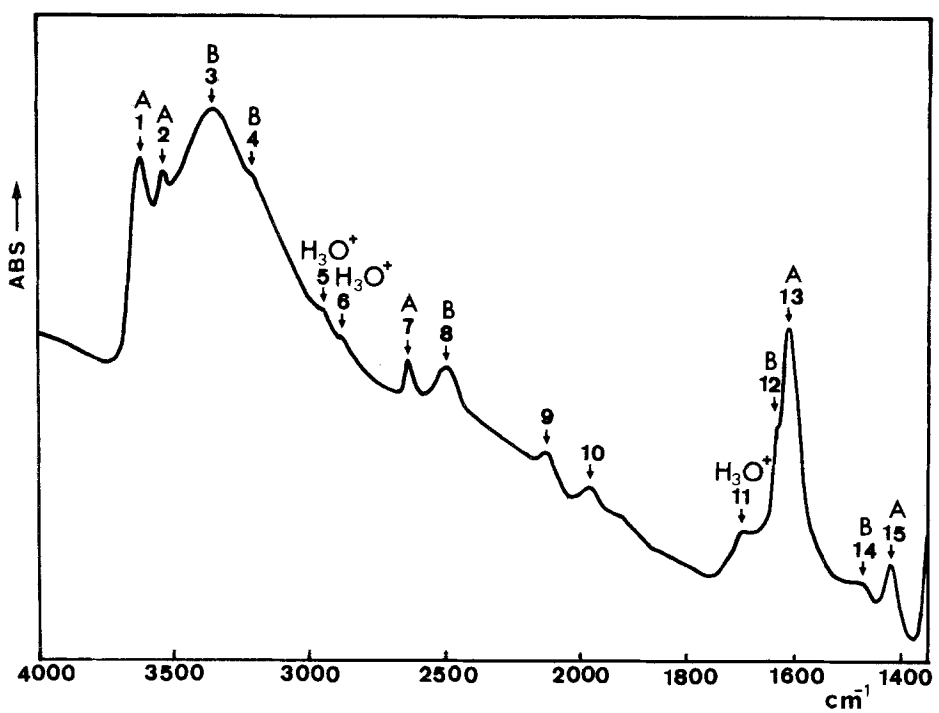

Fig. 2. Infrared spectrum (1400–4000 cm^{-1}) of partially deuterated $VOPO_4 \cdot 2H_2O$. Band assignments: 1, ν_{as}(OH); 2, ν_s(OH); 3, ν_{as}(OH); 4, ν_s(OH); 5, ν_{as}(OH); 6, ν_s(OH); 7, ν(OD); 8, ν(OD); 9, ν(VO—H); 10, δ(HOH) + L(motion); 11, δ(HOH); 12, δ(HOH); 13, δ(HOH); 14, δ(HOD) and 15, δ(HOD). A, B = A and B type water molecules.

possible vibrational coupling between δ(HOD) bands [28]. Syntheses of partially deuterated $VOPO_4 \cdot 2H_2O$ carried out in an aqueous solution having 10% of HOD led to the same results. Figure 2 shows the more significant spectral zone. From Figure 2 it can be noted: (a) there are two broad δ(HOD) bands owing to the two types of water molecules; and (b) the broadness of these unresolved bands argues strongly in favour of the existence of more than one δ(HOD) vibration for both water molecule types [28]. Thus, a C_s local symmetry can reasonably be assumed in both cases. Otherwise, according to the results on the band dichroism, the pseudo-C_2 axis of all coordinated and inserted water molecules will make an angle with the crystallographic z axis [29].

3.4.4. *Evidence for the Presence of $H^+(H_2O)$ Ions in the Interlayer Space*

A relevant aspect of the IR spectra of the dihydrate and the reduced phases, not yet discussed, is the presence of a set of bands appearing around 2940, 2870 and 1695 cm^{-1} (see Table IV and Figure 2). In particular, the band at 1695 cm^{-1} is clearly present also in the spectrum reported in [13], but remained unassigned. It has been claimed that this band, is a 'fingerprint' for H_3O^+ [30]. In a more recent paper, Corma and coworkers agree with the assignment of this band to the antisymmetric bending vibration of the H_3O^+ ion [31]. The bands at 2940 and 2870 cm^{-1} would be due to the antisymmetric and symmetric stretching vibrations of the H_3O^+ ion, respectively [30–32].

A general feature concerning these bands is their intensity decrease as the sodium intercalation degree increases. Besides this, an additional weak band at 2130 cm^{-1} can be noted. This band, whose intensity also decreases upon reduction, would be due to ν(VO—H) [21]. The presence of OH groups linked to vanadium atoms is required if there are H_3O^+ ions in the interlayer space. In fact, it might be thought that the more acidic coordinated water molecules of the solid $VOPO_4 \cdot 2H_2O$ are able to transfer one proton to inserted water molecules through an internal acid-base equilibrium such as:

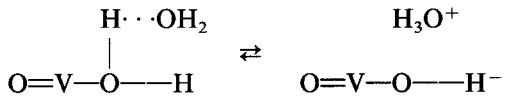

Such a schematic mechanism, suggested by the spectroscopic results [29], should be allowed by the hydrogen bonding network involving both A- and B-water molecule types (see above). Moreover, the intensity decrease of the H_3O^+ bands as the amount of intercalated sodium increases is consistent with the subsequent removal of coordinated acidic A water molecules. Thus, $VOPO_4 \cdot 2H_2O$ can be considered as a solid-acid.

3.5. DEHYDRATION/REHYDRATION PROCESSES

Figure 3a illustrates the time dependence of the IR spectrum of a sample of Solid **I** when, settled on an Irtran plate, it is exposed to a thermal lamp. On the other hand, in Figure 3b, the evolution of the IR spectrum of anhydrous α_1-$VOPO_4$ is presented as a function of the time of exposure to wet air. From these, it becomes evident that dehydration and rehydration proceed in very different ways. Thus, whereas dehydration involves two consecutive stages (as indicated also by the thermal analysis (see Section 3.2)), rehydration occurs with simultaneous occupancy of both kinds of crystallographic water sites.

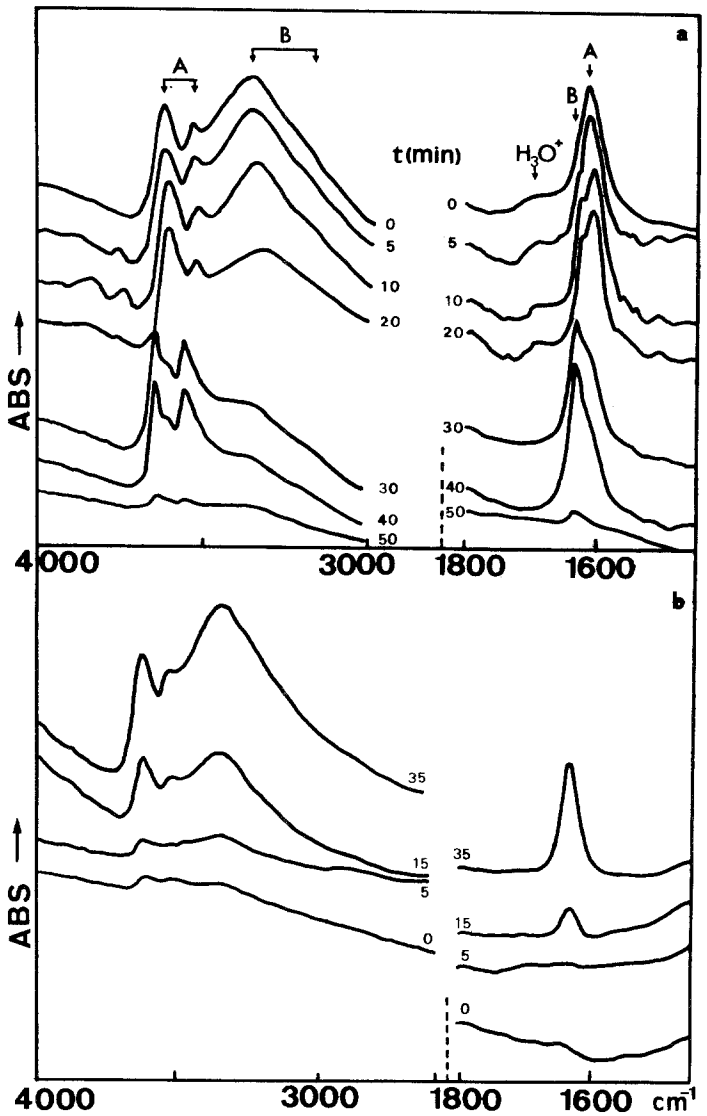

Fig. 3. Evolution of the infrared spectrum of Solid **I** (1400–4000 cm^{-1}). (a) Dehydration, (b) Rehydration.

Notwithstanding, it must be stressed that the bands due to B water molecules do not fully vanish until dehydration is complete. So, as pointed out above, in no case can a monohydrate containing only coordinated water be isolated. Otherwise, upon heating, the band at 1695 cm^{-1} (antisymmetric bending of H_3O^+) is readily lost.

The deintercalation/intercalation (dehydration/rehydration) processes have been also studied by variable temperature X-ray diffraction analysis. This study has been carried out on the dihydrate (Solid **I**) and on the reduced phases (Solids **II–VI**). The tendency of the samples to show preferential orientation allowed us to obtain simplified patterns in which the evolution of the (001) peaks with temperature can be followed (Figure 4).

Figure 4a shows schematically the variation of the (001) and (002) peaks of the Solid **I** (see Table III). It can be noted: (a) the dihydrate ($d = 7.45$ Å) is the only phase present

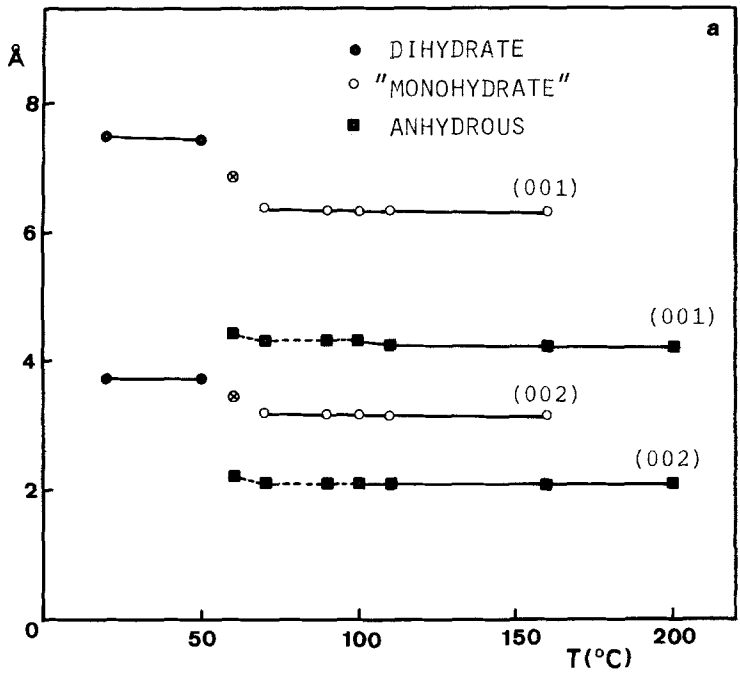

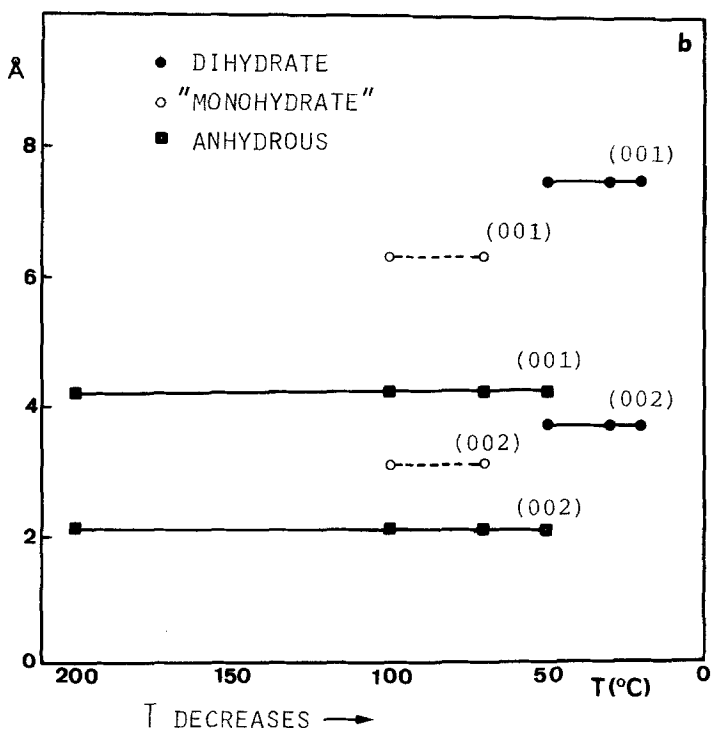

Fig. 4. Evolution of the (001) peaks in the X-ray powder diffraction pattern of Solid I. (a) Dehydration, ⊗ New metastable monohydrate phase. (b) Rehydration. Dotted lines denote minority phases.

below 50°C [33]; (b) at 60°C, a phase having a well defined interlayer space – equal to 6.88 Å – is observed together with the beginning of the formation of an essentially anhydrous phase ($d = 4.43$ Å); (c) between 70 and 160°C, two phases, namely the so called 'monohydrate' ($d = 6.37$–6.30 Å) and the anhydrous α_I-$VOPO_4$ ($d = 4.43$–4.23 Å), coexist. In this temperature range, the 'monohydrate' is the prevailing phase; and (d) above 160°C, only the anhydrous phase ($d = 4.23$ Å) remains [2]. Thus, the 'monohydrate' never appears as a single phase. In contrast, as shown in Figure 4b, when the resulting anhydrous phase is allowed to cool down in air, there is a rather sharp cut (around 50°C) between the anhydrous and dihydrate phases. Although indicated in the plot, peaks due to the 'monohydrate' have very low intensity and the (001) reflection is very poorly defined. Rehydration occurs therefore in a single step without appreciable 'monohydrate' formation.

Concerning the dehydration process, the formation of an intermediate phase whose interlayer space ($d = 6.88$ Å) lies between that corresponding to the dihydrate ($d = 7.45$ Å) and that reported in the literature for the 'monohydrate' ($d = 6.30$ Å) is a remarkable feature. The analysis of this sample reveals that it contains one water molecule, a result consistent with the simultaneous apparition of the anhydrous phase. We therefore observe a new metastable monohydrate phase. In fact, according to Section 3.4, the dihydrate–'monohydrate' transition would require, besides water removal, a change in the orientation of the coordinated water molecules. If this orientation were basically maintained in a first dehydration step leading to the metastable phase, then the rearrangement (thermally induced) of the A water molecules to become oriented with the pseudo C_2 axis perpendicular to the layers (in the resulting 'monohydrate') would involve a shortening of the interlayer space. Finally, the fact that both (001) and (002) peaks are always well defined for the 'monohydrate' whereas (001) peaks for the anhydrous phase are poorly defined below 160°C indicates that the 'monohydrate'–anhydrous conversion is accountable in terms of the domain model – which has allowed the explanation of the staging in related systems [34, 35]. On the other hand, rehydration of α_I-$VOPO_4$ layers must involve a cooperative steady movement of water molecules to occupy both crystallographic site types [13].

General features of the dehydration/rehydration processes involving reduced phases are analogous to the above. All phases retain their hydration water molecules until *ca.* 60°C [33] and the only remaining phases above *ca.* 200°C are the anhydrous ones. In the transition range, one intermediate hydrate coexists with the anhydrous phase, but no metastable phase has been observed. Anhydrous derivatives rehydrate readily (in a single stage) in air. As a significant result, it can be pointed out that the interlayer space in the anhydrous phases decreases as the intercalated sodium content increases (ranging from 4.30 – Solid **II** – to 4.02 Å – Solid **V**). Thus, it seems that sodium ions maintain their 'pillar' role. Otherwise, if the anhydrous derivatives are heated above *ca.* 500°C, a phase transition occurs (as shown by X-ray and DTA data) and the resulting solids do not reabsorb water.

To finish this discussion, we have approached the study of the formal kinetics of the dehydration and rehydration processes using thermogravimetric data. The values of the kinetic parameters listed in Table V have been estimated firstly from the mathematical approach of Abou-Shaaban and Simonelli (thus obviating the actual nature of the formal mechanism) [36]. Then these parameters have been used as reference criteria for elucidation of the formal mechanism type by non-isothermal procedures (applied to the same data set) using the Satava's integral method [37] to analyze the more widely assumed

Table V. Kinetic parameters

	1st Stage					2nd Stage				
	Abou-Shaaban		Satava			Abou-Shaaban		Satava		
Solid	$\Delta H^{\neq}$	Z	$\Delta H^{\neq}$	Z	Model*	$\Delta H^{\neq}$	Z	$\Delta H^{\neq}$	Z	Model*
I	21	10^{10}	19	10^{8}	R_3	21	10^{9}	19	10^{7}	R_3
III	15	10^{6}	12	10^{4}	F_1	11	10^{3}	13	10^{3}	R_1
IV	15	10^{6}	14	10^{5}	F_1	12	10^{3}	12	10^{3}	R_1
II	16	10^{6}	17	10^{7}	F_1	12	10^{3}	12	10^{3}	R_1
V	39	10^{20}	43	10^{22}	D_1	31	10^{13}	33	10^{13}	R_2

* Sharp's notation [42].

models for the kinetic study of solid state reactions [38]. In the case of Solid **I**, for which the first dehydration stage is, very likely, a step-by-step process, an isothermal additional experiment has been required [39, 40]. To shorten the discussion, only values provided by the models leading to the best fit have been included in Table V.

From Table V, three different dehydration patterns are shown: (a) in the case of Solid **I**, the rate-controlling process in the elimination of both water molecules is the reaction at the phase-boundary (R_3 model); (b) all three solids containing intermediate sodium amounts (Solids **II–IV**) behave similarly: B water elimination obeys the Avrami-Erofe'ev equations (random nucleation, F_1 model) [42] and the rate of the A water evolution is phase-boundary controlled (R_1 model); and (c) Solid **V**, having a high (although defective) amount of sodium, loses B water through a diffusion-controlled reaction (D_1), but A water evolution is again phase-boundary controlled (R_2 model). The following statements can be made: (a) the elimination of both water molecules (A and B) in the dihydrate (Solid **I**) occurs by the same formal mechanism. Thus, the fact that the activation enthalpy in the two stages is equal is evidence for the robustness of the hydrogen bonding network in the dihydrate; (b) sodium intercalation would involve local breakdowns of the hydrogen bonding network. As result, local nucleation and grain growth becomes determinant in the first dehydration stage, but the activation enthalpy decreases correspondingly; (c) in contrast, the presence of protons in Solid **V** would cause local reinforcement of hydrogen bonds. At the same time, the high sodium content might hinder the loss of the B water. In fact, this stage is diffusion controlled and the activation enthalpy increases significantly; and (d) as can be noted, the rate-controlling process in the elimination of the coordinated water is always the reaction at the phase-boundary. The evolution of the activation enthalpy (see Table V) may be thought of as a result of the change from the bulk phenomenon (Solid **I**, R_3 model) to a 'local' one (Solids **II–V**, R_1 model), whereas the presence of protons (as P—OH groups, see above) in Solid **V** is again shown by the high $\Delta H^{\neq}$ value.

Additionally, the formal kinetics of the rehydration of a sample of Solid **I** (resulting from the dehydration carried out at 2.2°C min^{-1} of Solid **I**) was studied. After cooling of the anhydrous phase (1.1°C min^{-1}) an isothermal experiment was performed at 20°C under a humidified N_2 atmosphere. When $\ln[-\ln(1-x)]$ is plotted as a function of $\ln(t)$ [42], the straight line $\ln[-\ln(1-x)] = -5.95 + 1.06\ln(t)$ (correlation coefficient = 0.998) is obtained. Accordingly, a three-dimensional phase boundary model (R_3) can be inferred for this single-stage process [42].

A remarkable feature is the coincidence in the formal mechanism for the rehydration and the two dehydration stages of Solid **I**. The above statement on the 'simultaneous' cooperative occupation of both crystallographic site types during the rehydration finds new support in this result.

4. Concluding Remarks

Figure 5 illustrates a structural proposal for the limit phases $Na_{0.25}V(IV)_{0.25}V(V)_{0.75}OPO_4 \cdot 1.75H_2O$ (5a) and $Na_{0.50}V(V)_{0.50}V(IV)_{0.50}OPO_4 \cdot 1.50H_2O$ (5b). Unit cells and space groups are based on X-ray powder diffraction patterns, although those of the sesquihydrate have been inferred by extrapolation. This has been done by considering the convergence suggested by Figure 1, even though experimental errors and the possible structural disorder in the limit phases obtained might introduce some uncertainty on the convergence point. The orthorhombic–tetragonal change may proceed through the progressive reduction of vanadium atoms in alternate planes. From Figure 5, it can be understood how the incoming sodium would cause the shortening of the c_r parameter and the elongation of a_r [by sequential substitution of A water along the (100) direction], whereas the b_r parameter would remain essentially unchanged.

From another point of view, the presence of H_3O^+ ions allows us to consider $VOPO_4 \cdot 2H_2O$ as a Bronsted acid [$VOPO_4 \cdot 2H_2O \rightleftarrows {}^-(HOVO)PO_4(H_3O)^+$] capable of yielding V(V) salts like the 'AHVPO$_6$' (A = NH_4^+, K^+, Rb^+, CS^+) reported by Pulvin and

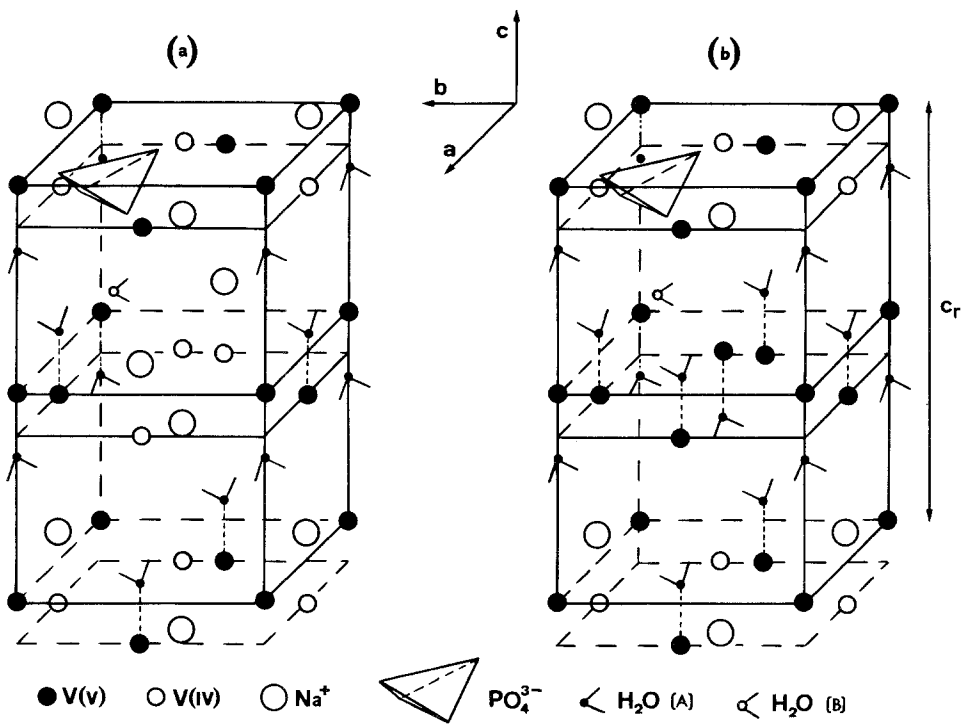

Fig. 5. Schematic view of the proposed unit cell for (a) $Na_{0.50}V^{IV}{}_{0.50}V^{V}{}_{0.50}OPO_4 \cdot 1.50H_2O$ (tetragonal, $P4_2mc$) and (b) $Na_{0.25}V^{IV}{}_{0.25}V^{V}{}_{0.75}OPO_4 \cdot 1.75H_2O$ (orthorhombic, *Pmma*). For clarity only one PO_4^{3-} group and one B-water molecule are shown in each unit cell.

Bordes [21]. On the other hand, the Lewis acid strength of the vanadyl(V) group, which results in the formation of coordination intercalates [9, 14], would be lowered in those sites in which vanadium atoms become reduced. Indeed, it is well known that vanadium atoms are frequently pentacoordinated in (VO^{2+}) containing derivatives [43]. This and the local charge neutralization tendency combine to fix the sodium location in the reduced phases.

Finally, it can be said that the inaccuracy in the literature data referring to the 'monohydrate' could be due to the simultaneous formation of the anhydrous phase and/or to the appearance of the new metastable phase here reported.

In order to check the proposal advanced, a structural study from powder X-ray data is in progress.

Acknowledgements

We very much thank the CAICYT for partial financial support of this research and A. J. Jacobson for helpful discussion.

Notes and References

1. E. Bordes and P. Courtine: *J. Chem. Soc. Chem. Commun.*, 294 (1985).
2. E. Bordes, P. Courtine, and G. Pannetier: *Ann. Chim.* **8**(2), 105 (1973).
3. T. P. Moser and G. L. Schraeder: *J. Catal.* **92**, 216 (1985).
4. D. Ballutaud, E. Bordes, and P. Courtine: *Mat. Res. Bull.* **17**, 519 (1982).
5. M. Tachez, F. Theobald, and E. Bordes: *J. Solid State Chem.* **40**, 280 (1981).
6. B. Jordan and C. Calvo: *Can. J. Chem.* **51**, 2621 (1973).
7. R. Gopal and C. Calvo: *J. Solid State Chem.* **5**, 432 (1972).
8. J. W. Johnson, D. C. Johnston, A. J. Jacobson, and J. F. Brody: *J. Am. Chem. Soc.* **106**, 8123 (1984).
9. J. W. Johnson, A. J. Jacobson, J. F. Brody, and S. M. Rich: *Inorg. Chem.* **21**, 3820 (1982).
10. H. R. Tietze: *Aust. J. Chem.* **34**, 2035 (1981).
11. M. Tachez, F. Theobald, J. Bernard, and A. W. Hewat: *Rev. Chim. Min.* **19**, 291 (1982).
12. A. J. Jacobson, J. W. Johnson, J. F. Brody, J. C. Scanlon, and J. T. Lewandowski: *Inorg. Chem.* **24**, 1782 (1985).
13. C. R'Kha, M. T. Vandenborre, and J. Livage: *J. Solid State Chem.* **63**, 202 (1986).
14. M. Martinez, A. Jimenez, L. Moreno, and S. Bruque: *Mat. Res. Bull.* **20**, 549 (1985).
15. N. Casañ Pastor, D. Beltrán-Porter, and E. Martinez-Tamayo: 9 ème Journée d'Etude des Equilibries entre Phases, M. T. Clavaguera Mora (Ed), Univ. Autonoma de Barcelona (Spain), 77 (1983); N. Casañ, E. Martinez, A. Beltrán, and D. Beltrán: VIII Reunión Ibérica de Absorción, Facultad de Ciencias, Málage (Spain), 44 (1983).
16. V. G. Jander, K. F. Jahr, and H. Witzmann: *Z. Anorg. Allg. Chem.* **217**, 65 (1934).
17. A. C. Chapman and L. F. Thirwell: *Spectrochim. Acta* **20**, 937 (1964).
18. G. Ladwig: *Z. Anorg. Allg. Chem.* **338**, 2 (1965).
19. J. Tudo and C. Carton: *Comp. Rend. Acad. Sci. Paris C* **289**, 219 (1979).
20. Y. E. Gorbunova and S. A. Linde: *Dokl. Akad. Nauk. SSSR* **245**, 584 (1979).
21. S. Pulvin, E. Bordes, M. Ronis, and P. Courtine: *J. Chem. Res. (S)* **29** (1981).
22. N. Casañ, E. Martinez, P. Amorós, N. Castelló, C. Llorente, A. Beltrán, and D. Beltrán: XXIV International Conference on Coordination Chemistry, Athens (Greece), August (1986).
23. M. R. Antonio, R. L. Barbour, and P. R. Blum: *Inorg. Chem.* **26**, 1235 (1987).
24. K. Nakamoto: *Infrared Spectra of Inorganic and Coordination Compounds*, 130–139, John Wiley & Sons, 4th Ed. (1986).
25. G. C. Pimentel and C. H. Sederholm: *J. Chem. Phys.* **24**, 639 (1956).
26. M. Falk: *Spectrochim. Acta A* **40**, 43 (1984).
27. S. Bruque, M. Martinez-Lara, L. Moreno-Real, A. Jimenez-Lopez, B. Casal, E. Ruiz-Hitzky, and J. Sanz: *Inorg. Chem.* **26**, 847 (1987).
28. M. Falk and O. Knop: *Water: A Comprehensive Treatise* Vol. 2, (F. Franks, Ed.), Chap. 2, Plenum Press, New York (1973).

29. While revising this article, A. Schneider (Thèse Doctoral, Université de Bordeaux I, France, October 1987) has reported results from a variable temperature solid-NMR (^1H and ^{31}P) study on $VOPO_4 \cdot 2H_2O$. It is shown that the interprotonic axis of inserted water molecules (type B) is tilted by 45–60° from the z axis. Otherwise, protonic exchange between A and B water molecules (activation energy = 0.08 eV) is observed.
30. L. J. Basile, P. Labonville, J. R. Ferraro, and J. M. Williams: *J. Chem. Phys.* **60**, 1981 (1974).
31. A. Corma, A. Lopez Agudo, and V. Fornés: *J. Chem. Soc. Chem. Commun.* 942 (1983).
32. R. Savoie and P. A. Giguere: *J. Chem. Phys.* **41**, 2698 (1964).
33. Concerning the temperatures indicated here, it must be stressed that the sample is maintained at the stated value for at least 30 min. Of course, owing to the different geometry of the samples in each experiment, the temperature values in the X-ray device do not coincide with those measured through the thermal study.
34. M. S. Whittingham and A. J. Jacobson: *Intercalation Chemistry* (Eds. M. S. Whittingham and A. J. Jacobson) Academic Press, New York (1982).
35. U. Costantino: *J. Chem. Soc. Dalton Trans.* 402 (1979).
36. R. R. A. Abou-Shaaban and P. Simonelli: *Thermochim. Acta* **26**, 67 (1978); **26**, 89 (1978).
37. V. Satava: *Thermochim. Acta* **2**, 423 (1971).
38. S. F. Hulbert: *J. Br. Ceram. Soc.* **8**, 11 (1979).
39. E. Martinez-Tamayo, A. Beltran-Porter, and D. Beltran-Porter: *Thermochim. Acta.* **98**, 167 (1986).
40. E. Martinez-Tamayo, A. Beltran-Porter, and D. Beltran-Porter: *Thermochim. Acta* **98**, 175 (1986).
41. J. H. Sharp, G. W. Brindley, and N. N. Achar: *J. Am. Ceram. Soc.* **47**, 379 (1966).
42. J. D. Handcock and J. H. Sharp: *J. Am. Ceram. Soc.* **55**, 74 (1972).
43. J. Selbin: *Chem. Rev.* **65**(2), 153 (1965).